Point-to-point radio link variation at E-band and its effect on antenna design

Point-to-point Radio Link Variation at E-band and Its Effect on Antenna Design

A. N. H. Al-Rawi, A. Dubok, M. H. A. J. Herben, and A. B. Smolders
Electromagnetics Group, Department of Electrical Engineering
Eindhoven University of Technology, The Netherlands

Abstract— Radio propagation will strongly influence the design of the antenna and front-end components of E-band point-to-point communication systems. Based on the ITU rain model, the rain attenuation is estimated in a statistical sense and it is concluded that for backhaul links of 1–10 km, antennas with a gain of 49.5 dBi are required. Moreover, depolarization can be a limiting factor for backhaul systems that are employing orthogonal polarization in order to improve capacity. Antenna mast movement becomes a relevant problem due to the narrow beamwidth of the high gain antennas, which is around 0.7°. We propose to implement a focal plane array as feed for the parabolic reflector antenna. This is to tackle the mast movement by electronic beam steering and to increase EIRP by increasing the number of active antenna elements, and to assist the mechanical alignment during installation.

1. INTRODUCTION

The network architectures of LTE and LTE-advanced promise the mobile users a wired experience in their wireless network. This puts high demands on the capacity (bits/sec) of the backhaul of these cellular systems. Fiber optics can due to its virtually unlimited capacity (10 s of Gbps) fulfill these demands. However laying optical fibers in an urban and rural area is very expensive, and therefore a wideband point-to-point radio link can be a good alternative. Millimeter-wave wireless systems operating in E-band (71–76, 81–86, 92–95 GHz), offer a bandwidth of 13 GHz which is sufficient to produce a bit rate of 1 Gbps with simple modulation schemes such as QPSK. This makes these systems a good option for the backhaul. There is an increasing demand on extending the E-band backhaul range. This is to reduce the construction and maintenance cost. It relies on increasing the antenna gain. As a consequence, the unwanted movement of the antenna mast becomes very relevant at this band because it causes a drop in the SNR. In addition, the antenna alignment during installation becomes cumbersome.

2. POINT-TO-POINT LINK VARIATION

The atmospheric window at E-band shows very low attenuation whereas it is significantly high at the neighboring 60 GHz band due to oxygen absorption [1]. Therefore, the 60 GHz band is limited to indoor and short range applications. The free-space and rain attenuation is high at E-band and they become very significant on the extended range of 10 km. These effects have been considered in [2].

Based on the ITU rain model [3] and data [4, 5] we analyzed the effect of rain in a statistical sense (see Fig. 1). For a backhaul length of 5 km, with rain attenuation of 0.01% of the time (i.e., 99.99% system availability); the total attenuation will be [A_{tot} = free-space 143.4 dB + rain attenuation 15.2 dB + atmosphere attenuation 4 dB = 162.6 dB]. A large antenna gain is required to compensate for such large attenuation. At an antenna gain of 41 dBi, a SNR at the receiver input of 40.4 dB, and with the assumption that the receiver has a noise figure of 10 dB, the SNR_d at the detector input is 30.4 dB. This is quite sufficient for QPSK with a bit error rate of 10^{-6}, that usually requires an SNR around 10 dB. For the longer path length of 10 km, the total attenuation is 179.5 dB, and SNR_d at the detector input is 16.5 dB. This is still adequate for the demodulator to accurately perform. Exceeding the rain attenuation of 0.01% to 0.001% of the time (i.e., 99.999% system availability) to increase the reliability of the point-to-point wireless communication, the total attenuation for 5 and 10 km path length is 175 dB and 195 dB, respectively. The SNR_d for the 5 km path length is 21 dB whereas for the 10 km path length it is 1 dB. The latter can be improved by increasing the receiver antenna gain to 49.5 dBi. This brings SNR_d to 9.5 dB, which is sufficient for QPSK with a bit error rate of 10^{-6}. This also can be further improved by reducing the receiver noise.

In addition, and due to the anisotropic nature of the rain medium, a pure vertically-polarized wave will arrive at the receiver with a small horizontally-polarized field component. This effect

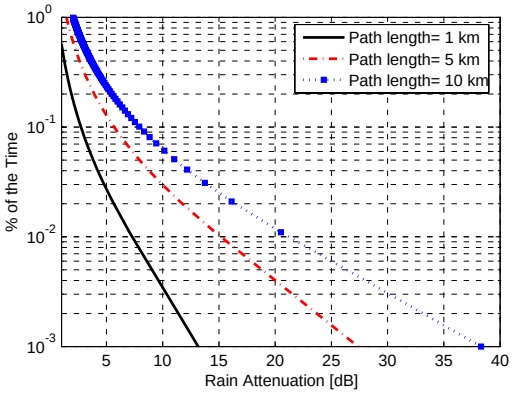

Figure 1: Fraction of the time versus the rain attenuation.

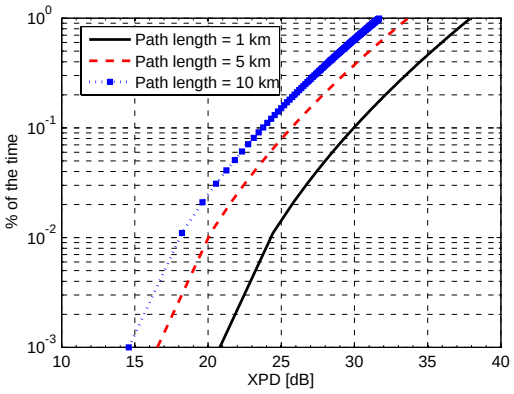

Figure 2: Fraction of the time versus cross polar discrimination.

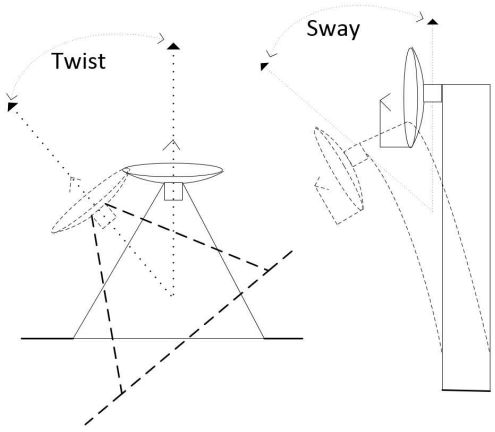

Figure 3: The motion of the antenna mast as twist and sway.

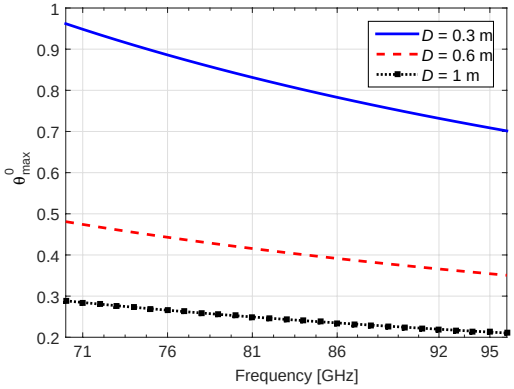

Figure 4: Maximum allowed twist/sway.

causes co-channel interference and due to that the channel capacity of wireless communication systems employing orthogonal polarization in order to double the capacity will be reduced. The depolarization is commonly quantified by the reduction in the cross-polar discrimination (XPD). The minimum XPD occurring during 0.01% of the time is related to the rain attenuation exceeded during 0.01% of the time. Most models and the standard ITU model [3] use this fact to estimate the XPD. As shown in Fig. 2, a shorter path length, i.e., 1 km has larger cross-polarization discrimination as compared to the longer ones. Moreover, reducing 0.01% of the time to 0.001% will reduce the cross-polarization discrimination. At 0.001% of the time the XPD can drop to 15 dB at a path length of 10 km.

The vertical gradient of the atmosphere refractive index can cause variation on the angle-of-departure and -arrival. However, based on the ITU model and data [6], these variations are not so significant for a path length of 1 or 10 km. For instance, the variation for 0.001% of the time is 0.09 degree for a 10 km path length. This is quite small as compared to the beamwidth of a typical high-gain E-band antenna (0.7°–1.2°).

The movement of the antenna mast is very relevant because high-gain antennas with small beamwidths are used for E-band backhaul systems. This motion is best described as twist and sway of the antenna mast, and illustrated in Fig. 3. This is mainly happening when the wind blows. Due to mast movement the propagating wave will no longer leave/enter the transmit/receive antenna at the maximum of its radiation pattern. This leads to an additional attenuation. The radiation pattern of the parabolic reflector antenna is used to estimate the −3 dB beamwidth. This estimation is repeated for three reflector diameters. The −3 dB point will set the specification on the maximum allowed twist and sway. Sway and twist exceeding the corresponding values in Fig. 4 will cause a significant degradation of the communication link. The wind forces can cause twist or sway up to 1 degree.

3. E-BAND ANTENNA DESIGN

The proposed configuration consists of a symmetrical reflector antenna and a focal plane array (FPA) as the feed antenna. This configuration is depicted in Fig. 5. The selected diameter is 95λ (i.e., 0.4 m) and delivers a maximum gain of 49.5 dBi at 71 GHz. The selected diameter is needed in order to compensate the total attenuation for the extended range of 10 km. The antenna gain is limited by the FCC regulation for E-band [7]. The configuration is modeled by using physical optics (PO) and a plane wave incident to the reflector antenna [8, 9]. The encircled power analysis [10, 11] is then applied in the focal plane to estimate the FPA size as a function of F/D, scan angle, and antenna efficiency. The efficiency here is the available power on the surface of the FPA disk normalized by the power captured by the reflector. The required scan angle is $+/-5$ degree, this is to track the mast movement and to assist the mechanical alignment. Due to the mast motion (twist and sway), the main beam is moving within a cone, therefore the topology of the FPA is chosen to be a circular disk.

In Fig. 6 the efficiency as function of FPA size is plotted for practical F/D ratios, and at the maximum required scan angle of 5°. An efficiency criterion of 80% criterion is used to select an appropriate F/D ratio and the FPA size. This criterion is to ensure high efficiency for the extended range of 10 km. $F/D = 0.6$ yields the smallest FPA size and this is important to minimise feed blockage. This means that the FPA has a 30 mm radius.

The trade-off is that the main beam in the focal plane is concentrated in a small region around the focal point (see Fig. 7). With the assumption that the antenna element spacing is equal to $\lambda = 2$. Practically, this limits the number of antennas to about 28 elements per scan angle (see Fig. 8). Therefore the EIRP can not be improved by exciting more array elements to create the beam. However, this can be improved by axially displacing the FPA in order to broaden the field

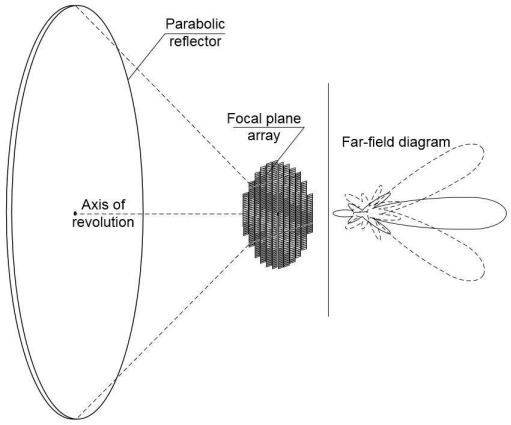

Figure 5: Artist impression of the FPA and reflector for point-to-point E-band wireless communications.

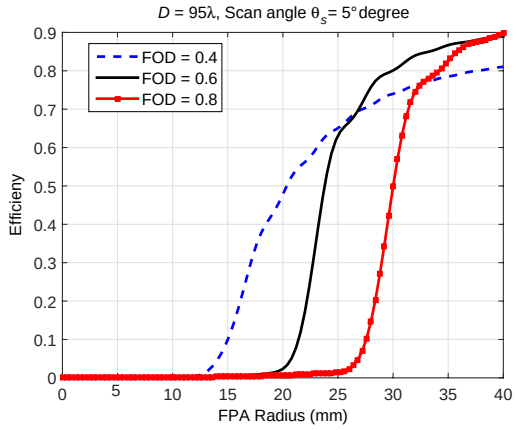

Figure 6: Encircled power analysis is applied in order to estimate the FPA size versus efficiency.

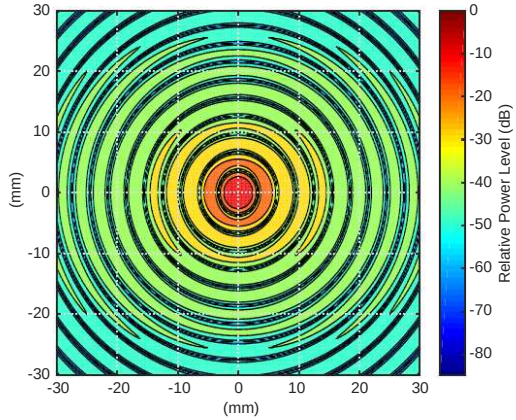

Figure 7: The field distribution image in the focal plane.

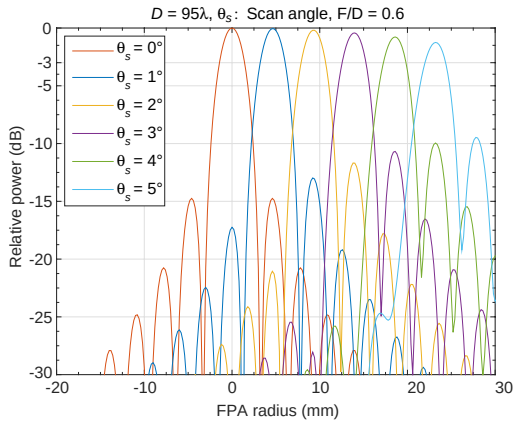

Figure 8: Cuts of the field distribution along the beam scan.

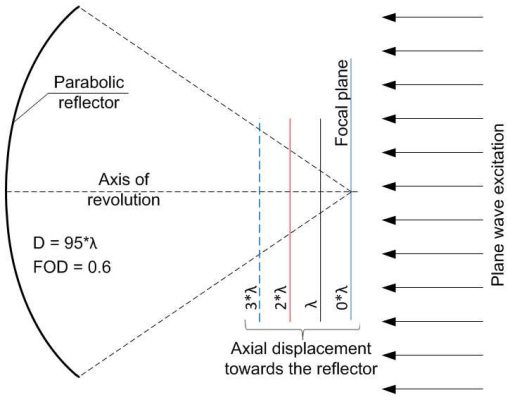

Figure 9: Axial displacement of the focal plane Model.

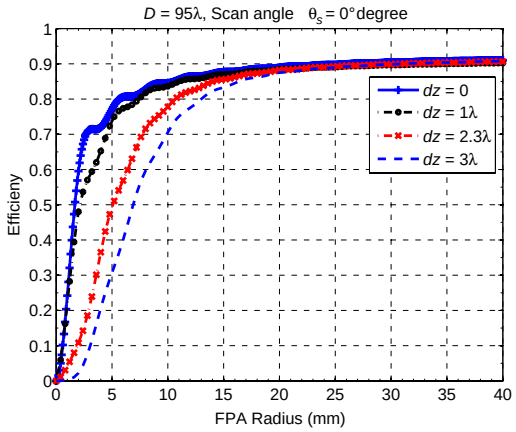

Figure 10: Efficiency versus FPA size for a range of axial displacements (dz). ($F/D = 0.6$).

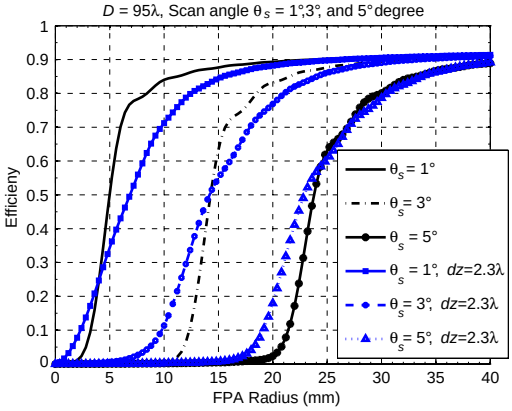

Figure 11: Efficiency of the axially displaced focal plane as a function of scan angle.

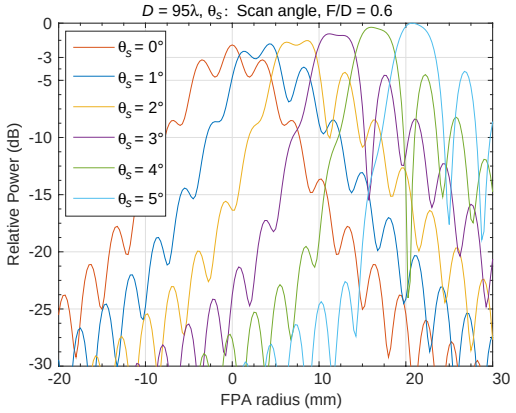

Figure 12: Cuts of the field distribution along the beam scan of the axially displaced plane.

distribution. The axial displacement (dz) is with λ steps towards the reflector as depicted in Fig. 9. 2.3λ is chosen as the optimum axial displaced focal plane. By exceeding it, the main bean of the focal plane pattern is going to be bifurcated. The efficiency curve of it is less steep and indicates the effects of broadening. Moreover, the 80% efficiency criterion still gives a small enough size of the FPA (see Fig. 10). In Fig. 12 the efficiency curves of the scan beam scenario, show a beam broadening up to 3°. Increasing the angle of incidence the effect of broadening is decreased because the scanned beam is getting narrower. We believe this is happening because of some focusing effect by the reflector. The beam broadening as shown in Fig. 12 indicates that the number of antenna elements can be increased significantly. About 78 elements will be involved up to 3° and to a less extent at 4° and 5°. Hence, EIRP can be improved and because of the overlap of the beams, array element reuse is possible.

4. CONCLUSION

High gain antennas at both the transmit and receiver site of the backhaul communication link are necessary to deliver acceptable levels of SNR. This is due to the rain attenuation and the large freespace attenuation. As a consequence of the high gain antenna requirement, the radiation pattern has a very narrow beamwidth. Due to this, the mast movement is very relevant. This problem has to be tackled, otherwise, additional attenuation will occur, resulting an outage. With the proposed antenna configuration of the FPA these issues can be overcome. The selected values of the reflector antenna diameter, F/D ratio, and FPA size are a good starting point for an optimized antenna design.

ACKNOWLEDGMENT

This work is supported by the Netherlands Foundation of Technical Sciences (STW).

REFERENCES

1. Rec. ITU-R P.676-6, "Attenuation by atmospheric gases," 2005.
2. Dyadyuk, V., J. D. Bunton, and Y. J. Guo, "Study on high rate long range wireless communications in the 71–76 and 81–86 GHz bands," *Proceedings of the 39th European Microwave Conference*, 2009.
3. Rec. ITU-R P.530-15, "Propagation data and prediction methods required for the design of terrestrial line-of-sight systems," 2013.
4. Rec. ITU-R P.838-03, "Specific attenuation model for rain for use in prediction methods," 2005.
5. Rec. ITU-R P.837-06, "Characteristics of precipitation for propagation modelling," 2012.
6. Rec. ITU-R P.453-10, "The radio refractive index: Its formula and refractivity data," 2012.
7. Federal Communications Commissions, "Allocation and service rules for the 71–76 GHz, 81–86 GHz, and 92–95 GHz bands," 2005.
8. Minnett, H. C., B. Mac, and A. Thomas, "Fields in the image space of symmetrical focusing refelctros," *Proceedings of the IEE*, Vol. 115, 1419–1430, 1968.
9. Ng Mou Keha, N. and L. Shafai, "Characterization of dense focal plane array feed for parabolic reflectors in achieving closely overlapping or widely separated multiple beams," *Radio Sci.*, Vol. 44, 2009.
10. Ivashina, M. V. and C. G. M. van't Klooster, "Focal field analyses for front-fed and offset reflector antenna," *2003 IEEE Antennas and Propagation Society Internationa Symposium*, Vol. 2, 750–753, 2013.
11. Hayman, D. B., T. S. Bird, K. P. Esselle, and P. Hall, "Encircled power study of focal field for estimating focal plane array size," *2005 IEEE Antennas and Propagation Society Internationa Symposium*, Vol. 3A, 371–374, 2015.